

respective antigens and may have potential as biomarkers of cell death. Further studies are required to define if these pharmacodynamic effects correlate with tumour responses and clinical outcome and whether these assays are also potential markers of drug induced toxicity.

144

POSTER

#### Novel Virtual Patient technology for predicting response of breast cancer and mesenchymal chondrosarcoma patients to mono- and combination therapy by cytotoxic and targeted drugs

L. Ziv<sup>1</sup>, L. Arakelyan<sup>1</sup>, R. Shohat<sup>1</sup>, M. Wick<sup>2</sup>, C. Webb<sup>3</sup>, D. Hankins<sup>4</sup>, D. Sidransky<sup>5</sup>, Z. Agur<sup>6</sup>. <sup>1</sup>Optimata Ltd, Ramat Gan, Israel; <sup>2</sup>CTRC Institute for Drug Development, San Antonio, TX, USA; <sup>3</sup>Van Andel Research Institute, Grand Rapids, MI, USA; <sup>4</sup>New Hope Pharmaceuticals Inc, Bethesda, MD, USA; <sup>5</sup>Johns Hopkins University School of Medicine, Baltimore, MD, USA; <sup>6</sup>Optimata Ltd and Inst. Medical Biomathematics, Ramat Gan, Israel

**Introduction:** Virtual Patient (VP) is a predictive biosimulation technology, comprising computer-implemented mathematical algorithms of key physiological, pathological and pharmacological processes in the body of the patient. Calibrated with available patient-specific data, the VP can accurately retrieve preclinical and clinical trials and predict short- and long-term effects of drugs.

**Materials and Methods:** The VP's solid tumor model was calibrated to retrieve the dynamics of breast cancer (BC) and mesenchymal chondrosarcoma (MCS) xenografts. Growth curves of untreated human tumor xenografts, derived from a lung metastasis of an MCS patient and histopathological results of this metastasis were used to create the MCS model. Published data served for modeling BC, PK/PD of three targeted therapies (Bevacizumab, Sunitinib, Sorafenib) and PK of four chemotherapeutics (Docetaxel, Gemcitabine, Doxorubicin and Irinotecan) in mice. *In vitro* proliferation assays of the MCS patient's tumor cells were used for establishing patient-specific concentration-effect curves for the chemotherapeutics. 'Administration' of the virtual drugs as single-agents and in combination was simulated and compared to corresponding experimental growth curves of treated and untreated MCS tumors for evaluating prediction accuracy. Optimal treatment was calculated.

**Results:** Significant superiority of Bevacizumab + Docetaxel combination, and Sunitinib, on other therapies, notably Gemcitabine, was shown for the MCS patient's xenografts. Over the simulated treatment period of up to 41 days, combinations with Bevacizumab are predicted to greatly enhance the treatment efficacy in comparison to the corresponding monotherapies in both cancer types. The average accuracy of the VP's predictions is 82%.

**Conclusions:** The VP showed high precision in predicting the growth pattern and response of xenografted MCS patient's tumor cells to various mono- or combination therapies. Our results suggest that, in general, treatments involving antiangiogenic drugs greatly improve MCS as well as BC tumor growth inhibition. In particular, Bevacizumab+Docetaxel regimens of reduced doses and inter-dosing intervals proved superior to other tested regimens for both indications. These results support the use of the Virtual Cancer Patient as a powerful tool for personalizing patients' treatment, especially when the application of new drugs is anticipated or when treatment of patients with rare diseases is considered.

## Drug delivery

145

POSTER

#### Marked therapeutic efficacy of a novel poly(ethylene-glycol) conjugated SN38 conjugate in xenograft models of breast and colorectal cancers

P. Sapra, C. Longley, Z. Zhang, H. Zhao, B. Rubio, M. Mehlig, J. Malaby, C. Conover, L.M. Greenberger, I.D. Horak. *Enzon Pharmaceuticals, Piscataway, USA*

**Background:** SN38 (10-hydroxy-7-ethyl-camptothecin) is the active metabolite of CPT-11 (Camptosar<sup>®</sup>). The clinical utility of SN38 has been severely limited due to its poor solubility. We have generated a novel water soluble conjugate, PEG-SN38, by linking SN38 with a multi-arm high molecular weight polyethylene-glycol (PEG). PEG-SN38 conjugate is readily soluble and has *in vitro* potency equivalent to that of the free drug on a panel of tumor cell lines. Here we evaluate the pharmacokinetics and therapeutic efficacy of PEG-SN38 in xenograft models of human breast and colorectal cancer.

**Material and Methods:** Therapeutic efficacy of PEG-SN38 was evaluated in nude mice implanted with MX-1 breast tumor fragments or HT-29 colorectal cells. Pharmacokinetics of PEG-SN38 was determined in naïve (tumor free) ICR mice.

**Results:** In the MX-1 breast model, treatment with either a single dose of 20 mg/kg or multiple doses of 5 mg/kg (q2d × 6) PEG-SN38 led to 100% tumor growth inhibition and complete cures of all the animals. At equivalent dose levels, treatment with CPT-11 caused a 26 and 44% TGI when given as a single dose or multiple injections, respectively. In the HT-29 colorectal xenograft model, treatment with a single suboptimal dose of 12 mg/kg PEG-SN38 caused a TGI of 47%, while CPT-11 at the same dose-level caused only a 3% TGI. In the same model, PEG-SN38 when given as multiple 3 mg/kg doses (q2d × 5) caused a TGI of 60% and treatment with PEG-SN38 was significantly better than that with CPT-11 or pegamotecan (a PEGylated prodrug of camptothecin) ( $P < 0.05$ ). The pharmacokinetic profile of PEG-SN38 in mice was biphasic showing a rapid plasma distribution phase during the initial 2 hrs followed by a 18–22 hrs terminal elimination half-life for the conjugate and a concomitant 18–26 hrs terminal elimination half-life for SN38.

**Conclusions:** PEG-SN38 demonstrated excellent antitumor activity in xenograft models of breast and colorectal cancer that, under our conditions, was significantly better than CPT-11. PEG-SN38 also provides a longer circulation half life compared to the native drug, SN38. These results merit further investigation of PEG-SN38 in the clinic.

146

POSTER

#### In vivo tumor targeting and radionuclide imaging with self-assembled nanoparticles: mechanisms, key factors, and their implications

D.H. Son<sup>1</sup>, S.A. Park<sup>1</sup>, S.W. Lee<sup>1</sup>, Y.W. Cho<sup>2</sup>, J.L. Roh<sup>1</sup>, S.Y. Kim<sup>1</sup>. <sup>1</sup>Univ. Of Ulsan College Of Medicine, Department Of Otolaryngology, Seoul, South Korea; <sup>2</sup>Univ. Of Ulsan College Of Medicine, Department Of Nuclear Medicine, Seoul, South Korea

**Background:** The development of more selective drug delivery systems is one of the most important goals of current anticancer research. We herein describe a highly effective tumor-targeting strategy utilizing self-assembled nanoparticles.

**Material and Methods:** By combining different hydrophobic moieties and hydrophilic polymer backbones, various self-assembled nanoparticles were prepared, and their *in vivo* distributions in tumor-bearing mice were studied by radionuclide imaging.

**Results:** The most striking result was that only one type of nanoparticles (fluorescein isothiocyanate-conjugated glycol chitosan (FGC) nanoparticles) among many nanoparticles exhibited highly selective tumoral localization while all the others showed poor tumor selectivity. Scintigraphic images obtained 1 day after the intravenous injection of FGC nanoparticles clearly delineated the tumor against adjacent tissues. The mechanisms underlying the tumor targeting with self-assembled nanoparticles were investigated in terms of the physicochemical properties of nanoparticles and tumor microenvironments. FGC nanoparticles were preferentially localized in perivascular regions, implying their extravasation to tumors through the hyperpermeable tumor vasculature. The magnitude and pattern of tumoral distribution of self-assembled nanoparticles were influenced by several key factors: (i) *in vivo* colloidal stability: nanoparticles should maintain their intact nanostructures *in vivo* for a long period of time, (ii) particle size, (iii) intracellular uptake of nanoparticle: fast cellular uptake greatly facilitates the tumor targeting, (iv) tumor angiogenesis: pathological angiogenesis permits access of nanoparticles to tumors.

**Conclusions:** We believe that this work can provide insight for the engineering of nanoparticles and be extended to cancer therapy and diagnosis, so as to deliver multiple therapeutic agents and imaging probes at high local concentrations.

147

POSTER

#### A new Taxol delivery system for the treatment of brain primary or metastatic tumors

R. Gabathuler<sup>1</sup>, M. Demeule<sup>1</sup>, A. Regina<sup>2,3</sup>, C. Che<sup>1</sup>, R. Beliveau<sup>2,3</sup>. <sup>1</sup>AngioChem Inc., Research and Development, Laval Quebec, Canada; <sup>2</sup>UQAM, Laboratory of Molecular Medicine, Montreal Quebec, Canada; <sup>3</sup>UQAM, Hopital St Justine, Montreal Quebec, Canada

**Background:** Brain tumors are among the most vascularized and resistant tumors. The blood-brain barrier (BBB) is frequently a rate limiting factor for the penetration of anticancer drugs into the central nervous system. In the present study, we investigated the utilization of a new peptide based drug delivery technology that provides a non-invasive and flexible platform for transporting drugs into the central nervous system. Taxol, which is normally impeded to reach its target in the brain by the presence of the P-glycoprotein (P-gp) efflux pump at the BBB, has been conjugated to these vector-peptides (Angiopeps). The efficacy of this Taxol-Angiopep conjugate has been assessed *in vitro* and *in vivo* using different experimental approaches.

**Material and Methods:** An *in vitro* model of the BBB and *in situ* brain perfusion were used to assess the brain uptake of Taxol-conjugate. Xenograft models of glioblastoma (U87) and non-small cell lung carcinoma (NCI-H460) were established by subcutaneous (s.c.) injections of cancer cells in immunodeficient mice nu/nu. Moreover, glioblastoma as well as lung brain metastasis models were also established by intracranial stereotaxic injections of U87 and NCI-H460 cells, respectively.

**Results:** We demonstrate here the transcytosis ability of peptides derived from kunitz domain called Angiopeps using an *in vitro* model of the BBB and *in situ* brain perfusion. Angiopep transcytosis across bovine brain capillary endothelial cell (BBCEC) monolayers is at least 19-fold higher than that of holo-transferrin. In addition, Taxol, has been conjugated to these vector-peptides (Angiopeps). Importantly, Taxol-Angiopep conjugate has a similar effect than free Taxol on cancer cell proliferation *in vitro*. However, the conjugation of Taxol to Angiopep allows to bypass P-gp leading to a higher accumulation of Taxol in the brain parenchyma. We also found that Taxol-Angiopep conjugate caused a stronger inhibition of the s.c. tumor growth of U87 and NCI-H460 than free Taxol. Moreover, Taxol-Angiopep conjugate significantly increased survival of mice implanted with intracranial NCI-H460 and U87 cells by 27 and 24%, respectively.

**Conclusion:** Overall, these results indicate that the conjugation of Taxol with Angiopep-vector increases the effect of Taxol on tumor growth as well as Taxol accumulation in brain. Furthermore, in primary and secondary brain tumor models, Taxol-Angiopep conjugate administration prolonged mice survival.

#### 148 POSTER Self-assembling nanoparticles targeting G-protein coupled receptors and ABC transporters

N. Tarasova. NCI-Frederick, Structural Biophysics Laboratory, Frederick, MD, USA

We have previously shown that synthetic analogs of the transmembrane domains (TMs) of G-protein coupled receptors (J Biol Chem 1999; 274(49): 34911–5) and of the multiple drug resistance protein, P-gp (J Med Chem 2005; 48(11): 3768–75) efficiently and specifically inhibit the function of the target protein. The remarkable feature of these inhibitors is that they can be designed rationally solely on the basis of the primary structure of the protein.

A transmembrane antagonist of CXCR4 incorporated in lipid liposomes was shown to completely inhibit metastasis in a mouse model of breast cancer. We have found recently that liposomes may not be needed for the delivery of TM antagonists.

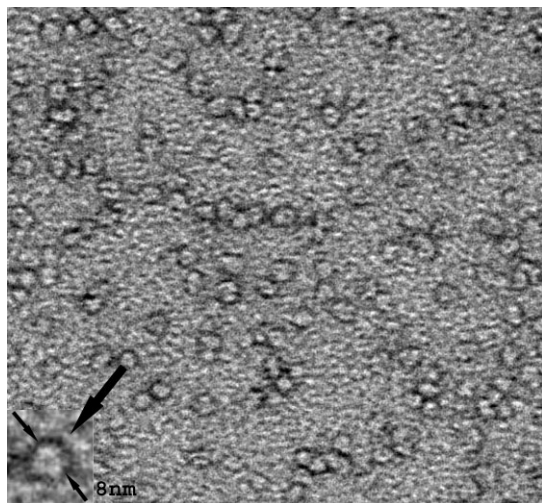


Fig. 1. Cryo-electron microscopy of the transmembrane antagonist of CXCR4 receptor CXCR4-2-2 demonstrated self-assembly of the compound into nanoparticles with a diameter about 8 nm.

Experiments utilizing multiple angle light scattering have shown that TM peptides self-assemble into stable nanoparticles in aqueous solutions. Cryo-electron microscopy has revealed formation of uniform particles with a diameter of about 8 nm, which is within the presumed optimal range for intra-tumor delivery. Electron microscopy studies of numerous "mutant" peptides have shown that negative charges added to the C-terminal end of the peptides were critical for formation of small uniform particles. Many TM peptide micelles aggregated further forming rings and strings. Addition of short polyethylene glycol chains reduced aggregation, while

PEG chain consisting of 39 repeats provided for non-aggregating and uniform nanoparticles. NMR, light scattering and calorimetry studies have demonstrated remarkable stability of TM peptide micelles with CCM in low micromolar range.

Nanoparticulate forms of transmembrane peptides retained full biological activity. CXCR4-targeting TM micelles inhibited signaling through the receptor, while ABCG2 and P-glycoprotein TM nanoparticles inhibited drug efflux mediated by the corresponding transporter. Nanoparticles formed by TM peptides also efficiently encapsulated poorly soluble hydrophobic drugs, thus providing a unique delivery system with dual anti-tumor activity. Self-association of transmembrane peptides in aqueous solutions is a novel phenomenon. It enables the development of new methods of specific and rational targeting of integral membrane proteins *in vivo* and provides for a new paradigm in drug development where the drug itself self-assembles in a nanostructure that has the desired size and surface properties for intra-tumor delivery.

#### 149 POSTER Pharmacokinetics of irinotecan and its metabolites after i.v. administration of IHL-305, a novel PEGylated liposome containing irinotecan, to tumor-bearing mice

A. Kurita, T. Furuta, N. Kaneda, I. Kato, S. Sawada, M. Onoue. Yakult Honsha Co., Ltd., Yakult Central Institute for Microbiological Research, Tokyo, Japan

**Background:** IHL-305 is a preparation of irinotecan encapsulated in PEGylated liposome. IHL-305 demonstrated stronger tumor growth inhibition effect than irinotecan hydrochloride (CPT-11) on various human cancer xenografts such as the colon, lung, gastric, ovarian, and prostate cancer cell lines. Liposome preparations are selectively transported to tumor tissues by the enhanced permeability and retention (EPR) effect. In this study, we compared the pharmacokinetics after i.v. administration of IHL-305 with CPT-11 in tumor-bearing mice.

**Materials and Methods:** Female BALB/c mice transplanted with Meth A tumors were i.v. administered with IHL-305 or CPT-11 at a dose of 16.7 mg/kg, and were exsanguinated at 8 time points until 96 hours after dosing, followed by extirpation of the tumor, liver and kidney. The concentrations of irinotecan and its metabolites, SN-38, and SN-38 glucuronide (SN-38G), in plasma and these tissues were measured.

**Results:** The plasma irinotecan, SN-38, and SN-38G concentrations peaked at 0.167, 6, and 12 hours after IHL-305 dosing, respectively, whereas those after CPT-11 dosing peaked at 0.167 hours. The  $AUC_{0-\infty}$ ,  $C_{max}$ , and  $t_{1/2}$  of irinotecan after IHL-305 dosing were higher than those after CPT-11 dosing (302-, 55-, and 2.9-fold, respectively). The  $C_{max}$  of SN-38 and SN-38G after IHL-305 dosing were lower than those after CPT-11 dosing (0.13- and 0.23-fold), however, the  $AUC_{0-\infty}$  were higher (2.5- and 1.8-fold), because of their much slower disappearance than CPT-11 dosing. Irinotecan and SN-38 concentrations in tumor tissue after CPT-11 dosing peaked at 0.167 and 0.5 hours, followed by a relatively rapid decrease. Concentrations after IHL-305 dosing remained nearly constant up to 12 hours for irinotecan and 48 hours for SN-38 and then decreased gradually. Their  $AUC_{0-\infty}$  were higher than those after CPT-11 dosing (9.02- and 3.89-fold). The  $AUC_{0-\infty}$  of irinotecan and SN-38 in the liver and kidney tissues after IHL-305 dosing were also higher than those after CPT-11 dosing (15- and 2.3-fold for the liver, and 4.1- and 2.4-fold for the kidney, respectively).

**Conclusion:** The irinotecan and SN-38 concentrations in plasma, tumor, liver, and kidney tissues after IHL-305 administration to tumor-bearing mice were markedly higher than those after CPT-11 dosing. The AUC ratio of SN-38 between CPT-11 and IHL-305 administration in tumor tissue was greater than in the liver and kidney, suggesting that targeting was improved by its liposomal formulation.

#### 150 POSTER Effects of dasatinib on the pharmacokinetics of simvastatin, a cytochrome P450 3A4 substrate, in healthy subjects

C.-Y. Wu, F. Callegari, K. Williams, A. Sanil, T. Griffin, A. Blackwood-Chirchir. Bristol-Myers squibb, Pharmaceutical Research Institute, Princeton, USA

**Background:** Dasatinib – an oral inhibitor of multiple oncogenic kinases – has demonstrated clinical efficacy in CML and Ph+ ALL. *In vitro* dasatinib inhibits CYP3A4 ( $IC_{50}$  = 1.9  $\mu$ M). The objective of this study was to assess the effect of dasatinib on simvastatin plasma concentration-time profiles in healthy subjects.

**Methods:** Healthy subjects (N=48) were treated in this open-label, randomized, two-period, two-treatment, balanced, crossover study. The treatments were: A) 80 mg simvastatin (single dose) (control); and B) 80 mg simvastatin plus 100 mg dasatinib (both single doses). Blood samples for